Physica Scripta. T92, 126–129, 2001

Z-Dependence of Photo-Emission Spectra for Highly Charged Neonlike Ions

D. Kato[1]*, N. Nakamura[1], S. Ohtani[1,2] and A. Sasaki[3]

[1] Cold Trapped Ions Project, ICORP, JST, Axis-Chofu bldg. 3F 1-40-2 Tokyo 182-0024, Japan
[2] Institute for Laser Science, University of Electro-Communications, Tokyo 182-8585, Japan
[3] Advanced Photon Research Center, Kansai Research Establishment, JAERI, Kyoto 619-0215, Japan

Received July 31, 2000; accepted October 9, 2000

PACS Ref: 31.15.Ne, 31.30.Jv, 32.30.Rj, 32.70.Fw, 32.80.Bx, 34.80.Kw

Abstract

Z-dependence of atomic properties for $n = 3$ excited states of highly charged neonlike ions was investigated theoretically for $Z = 50$–56. Configuration interaction effects for relativistic atomic states of three electric-dipole lines: 3D ($3d_{5/2} \rightarrow 2p_{3/2}$), 3E ($3d_{3/2} \rightarrow 2p_{3/2}$) and 3F ($3s_{1/2} \rightarrow 2p_{1/2}$), were examined in terms of *jK*-coupling. A present collisional-radiative model consistently explained intensity ratios for 3F/3D observed with the Tokyo-EBIT, and predicted a vanishing intensity for the 3E line near $Z = 52$. The vanishing intensity for the 3E line was attributed to the Cooper-minimum type mechanism.

Systematic study on atomic properties along an isoelectronic sequence is important to test atomic structure theories. The non-relativistic Z expansion theory with the lowest order relativistic corrections has long been a basis for understanding the Z-dependences of the atomic properties. However, in the very high Z region, the idea of the Z expansion becomes meaningless, since the expansion would involve all powers of Z. *Ab initio* fully relativistic calculations are therefore required in the very high Z region. As Weiss and Kim [1] pointed out, relativity split levels of a non-relativistic *LS*-coupled state into different large-Z asymptotes causing level crossing in an intermediate region. Kagawa *et al.* [2] performed fully relativistic configuration interaction calculations for the neonelike sequence. Their calculations predicted strong configuration mixing between $(2p_{3/2}^{-1}3d_{5/2})_{1-}$ and $(2p_{1/2}^{-1}3s_{1/2})_{1-}$ excited states at about $Z = 55$ where energy levels of the two excited states interchange. They found an anomalous redistribution of oscillator strengths in the two coupled states. Beiersdorfer [3] discussed about configuration interaction effects in the quantum electrodynamics contributions at the level crossing. Rice *et al.* [4] predicted another strong configuration mixing between excited states with different principal quantum numbers in the neonlike sequence, i.e. $(2p_{1/2}^{-1}6d_{3/2})_{1-}$ and $(2p_{3/2}^{-1}7d_{5/2})_{1-}$, and found the oscillator strength anomaly in the two states. Ivanova and Grant [5] investigated the oscillator strength anomalies in the neonlike sequence for applications to X-ray laser modeling. Recently, a further investigation on the level crossing has been made theoretically by Kitano and Kagawa [6] for forbidden transitions in the neonlike sequence.

In the present work, *ab initio* relativistic calculations of $n = 3$ energy levels of highly charged neonlike ions were performed for some prominent lines in X-ray spectra observed with the Tokyo-EBIT. A simple collisional-radiative model was implemented to calculate line intensities. The Z-dependence of atomic properties along the $n = 3$ electronic sequence was investigated with the present calculations and the experimental spectra.

Recently a set of X-ray spectra from highly charged neonlike ions ($Z = 50 - 56$) was measured with a flat crystal spectrometer at the Tokyo-EBIT [7]. Energies of some prominent lines due to transitions from $n = 3$ excited states to the ground state were precisely measured. We calculated the energies for three electric-dipole lines from $(2p_{3/2}^{-1}3d_{5/2})_{1-}$, $(2p_{3/2}^{-1}3d_{3/2})_{1-}$ and $(2p_{1/2}^{-1}3s_{1/2})_{1-}$ excited states by the multi configuration Dirac–Fock (MCDF) method. We refer to these three lines as 3D, 3E and 3F, respectively, in subsequent discussions, following Loulergue and Nussbaumer [8]. The lowest order quantum electrodynamics corrections: single transverse photon interaction, self-energy and vacuum polarization corrections, were taken into account through relativistic configuration interaction calculations with the MCDF orbital wavefunctions. The nuclear volume effect was represented by the Fermi model with 90–10% fall-off thickness $t = 2.3$ fm and root-mean-square radius of Johnson and Soff [9]. These calculations were implemented with the GRASP92 code [10]. The orbital wavefunctions for the ground state: $(2p^6)_{0+}$, and those for seven excited states: $(2l^{-1}3l')_{1-}$, were obtained by separate MCDF calculations, so that differences of screening effect in core orbital were taken into account. Figure 1 shows a comparison of the present calculations with other available experiments and relativistic many-body perturbation (RMBPT) calculations by Avgoustoglou *et al.* [11] for $Z = 50 - 92$ as well as the experiments at the Tokyo-EBIT. The agreement is very good for $Z < 60$; the largest discrepancy is estimated to be less than 0.04 %, though some of the present calculations are still out of very small experimental uncertainties. Very few measurements are available for $Z > 60$ with rather large uncertainties. For $Z > 60$ the RMBPT calculations are considerably larger than the present calculations. It is noted that the self-energy corrections to the excitation energies are affected by tiny differences of the screening effect in core orbitals for the large-Z region. The discrepancies of the two calculations are probably due to differences in the self-energy corrections. Precise experimental measurements are strongly desired for the high-Z region.

To simulate line intensities of the X-ray spectra obtained with the Tokyo-EBIT, we used a simple collisional-radiative model (CRM). In the EBIT, trapped ions are interacting

*e-mail: kato@hci.jst.go.jp

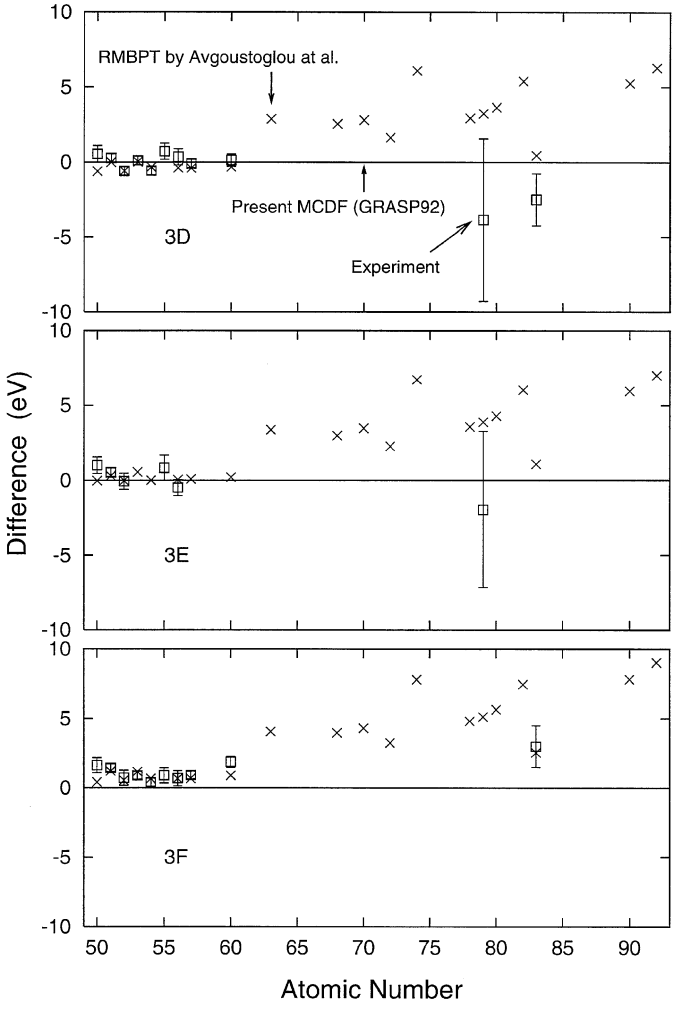

Fig. 1. Comparison of 3D, 3E and 3F energies with RMBPT calculations [11] and experiments. The experimental values from Ref. [12] are used for $Z = 54$ and 57, Ref. [13] for $Z = 79$, and Ref. [14] for $Z = 83$.

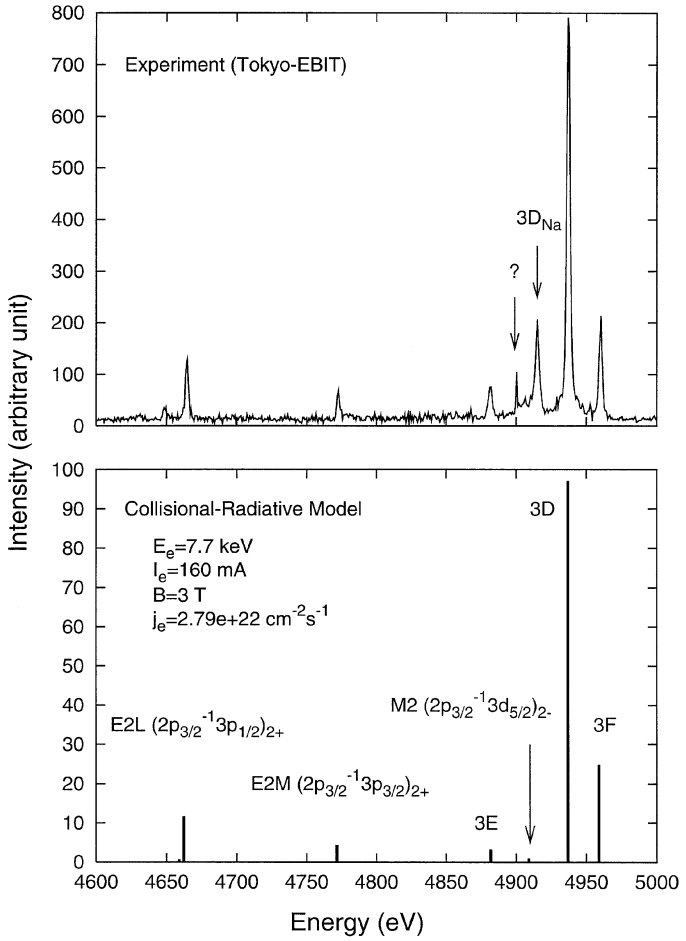

Fig. 2. X-ray Spectrum for the neonlike Ba^{46+} ion. The upper panel is a spectrum of the experiment at the Tokyo-EBIT, and the lower is a spectrum of the present CRM.

with an unidirectional electron beam which is compressed and confined by a magnetic field. In the present CRM, we assumed a uniform distribution for the current density of the electron beam in the interaction region. The electron beam radius in the interaction region was estimated by the Hermann theory [15]. According to experimental conditions at the Tokyo-EBIT (see Fig. 2), we estimated the electron beam current density to be of order $\sim 10^{22}\,\mathrm{cm}^{-2}\,\mathrm{s}^{-1}$. With such a low current density, collision rates are much smaller than radiation rates; most excited states immediately cascade to the ground state radiating photons before subsequent electron impact. Since the peak energy of the electron beam in the experiments is lower than the ionization threshold from the ground state of the neonlike ions, the fluorinelike or higher charge states cannot be created by a single collision with the electron beam. We therefore ignored contributions from the higher charge states. Since very small abundance of lower charge states was inferred from the relative intensities of the sodiumlike satellite lines observed in the experiments, contributions from the lower charge states were also neglected. Consequently, we omitted any charge changing process, i.e. ionization and recombination in the present CRM. Further, resonant excitations of the neonlike ions were neglected, since Auger decay branches are usually very small for highly charged ions.

In a stationary state for the present CRM, rate equations for populations in atomic levels, $\{N_\mathrm{i}\}$, are expressed as,

$$\left(\sum_{j\neq i}\Gamma^{\mathrm{col}}_{j\leftarrow i}+\sum_{j<i}\Gamma^{\mathrm{rad}}_{j\leftarrow i}\right)N_i=\sum_{j\neq i}\Gamma^{\mathrm{col}}_{i\leftarrow j}N_j+\sum_{j>i}\Gamma^{\mathrm{rad}}_{i\leftarrow j}N_j, \qquad (1)$$

where $\Gamma^{\mathrm{col}}[\mathrm{s}^{-1}]$ represents collisional excitation and de-exciation rate coefficients, and $\Gamma^{\mathrm{rad}}[\mathrm{s}^{-1}]$ represents radiative transition probabilities. The expression of Γ^{col} used in the present CRM is,

$$\Gamma^{\mathrm{col}} = j_\mathrm{e}\sigma(E_\mathrm{e}), \qquad (2)$$

where $j_\mathrm{e}[\mathrm{cm}^{-2}\mathrm{s}^{-1}]$ is the electron beam current density, and $\sigma(E_\mathrm{e})[\mathrm{cm}^2]$ is the electron impact excitation cross section at an electron energy of E_e. This means that the energy distribution of the electron beam is represented by a delta function, $\delta(E - E_\mathrm{e})$. The ground state and eighty-nine excited states: $2l^{-1}nl'(3 \leq n \leq 4)$, were included. All atomic data were obtained from the HULLAC code [16]. In practice, we solved an over-determined set of linear algebraic equations for relative populations, $\{N_\mathrm{i}/N_0\}(\mathrm{i} > 0)$, where N_0 represents the population in the ground state. A unique solution set to the over-determined system was readily obtained with the singular value decomposition method [17]. A simulated X-ray spectrum of the neonlike Ba^{46+} ion is shown in Fig. 2 together with the observed one. As seen in the figure, the present CRM consistently explains

relative intensities of lines observed in the experiment. Besides three prominent electric-dipole lines (3D, 3E and 3F in the figure), two electric-quadrupole lines (E2L and E2M in the figure) are also visible in both spectra.

The Z-dependences of peak energies and relative intensities are shown in Fig. 3 for $Z = 50 - 56$. For calculations of their energies, Z was treated as a continuously variable parameter. An apparent avoided crossing between the 3D and 3F energy levels is seen near $Z = 55$. Atomic states for the three lines have the same J and parity (Π) quantum numbers which are all constants of motion for relativistic atomic states without interactions with nuclear electro-magnetic moments. Their energy levels therefore never cross at any Z-parameter, otherwise each atomic state cannot be specified uniquely. In this aspect, the near-miss between the 3E and 3F energy levels near $Z = 51$ is rather intriguing suggesting another quantum number which further classifies the three atomic states in this Z region. By examining degrees of configuration mixing in the jK-coupling scheme [18], in this Z region we found that the three atomic states for the 3D, 3E and 3F lines were well represented by $(2p^{-1}3d)\frac{3}{2}\left[\frac{1}{2}\right]_{1-}$, $(2p^{-1}3d)\frac{3}{2}\left[\frac{3}{2}\right]_{1-}$ and $(2p^{-1}3s)\frac{1}{2}\left[\frac{1}{2}\right]_{1-}$, respectively, in $(2l^{-1}3l')j[K]_{J\Pi}$ notation. The K quantum number represents a coupling between an inner-shell total angular momentum j and an outer-shell orbital angular momentum l'. The degrees of the configuration mixing are shown in Fig. 4. The {3D, 3F} and 3E are therefore classified into two different K states: $K = \frac{1}{2}$ and $K = \frac{3}{2}$, respectively. According to ordinal quantum theories, the different K states weakly interact through small perturbations, while the same K states interact strongly at crossing points, since the K quantum number is approximately a good quantum number in this Z region. The near-miss between the 3E and 3F energy levels are therefore

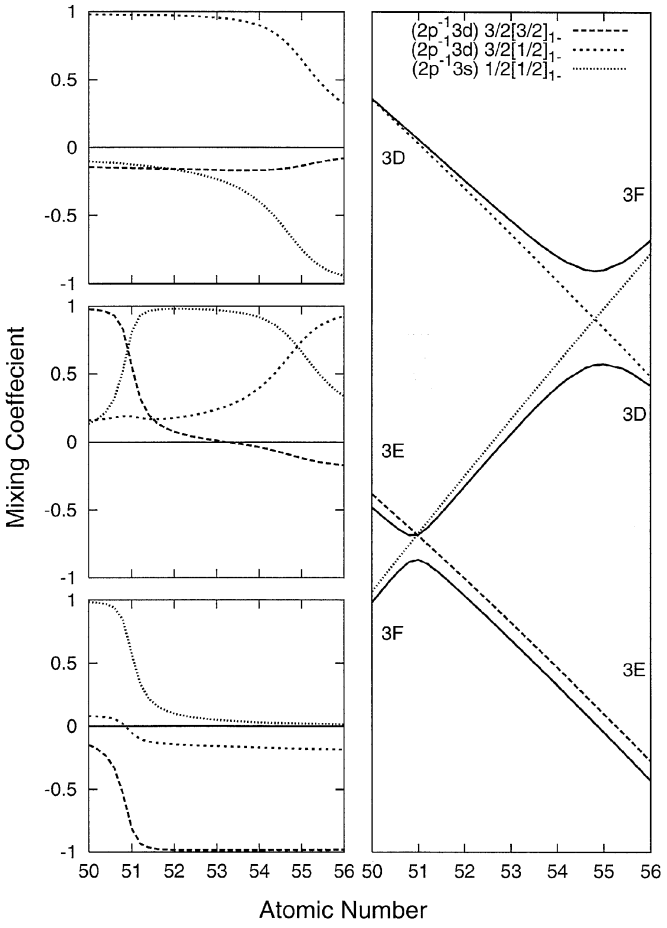

Fig. 4. The right hand panel shows Z change of energy levels for 3D, 3E and 3F lines. Solid curves represents eigen energies, long-dash curves $(2p^{-1}3d)\frac{3}{2}\left[\frac{3}{2}\right]_{1-}$ state energy, short-dash curves $(2p^{-1}3d)\frac{3}{2}\left[\frac{1}{2}\right]_{1-}$ state energy, and dotted curves $(2p^{-1}3s)\frac{1}{2}\left[\frac{1}{2}\right]_{1-}$ state energy. The three left hand panels represent degrees of configuration mixing. The upper panel is for the upper eigen state, the middle panel for the middle eigen state, and the lower panel for the lower eigen state.

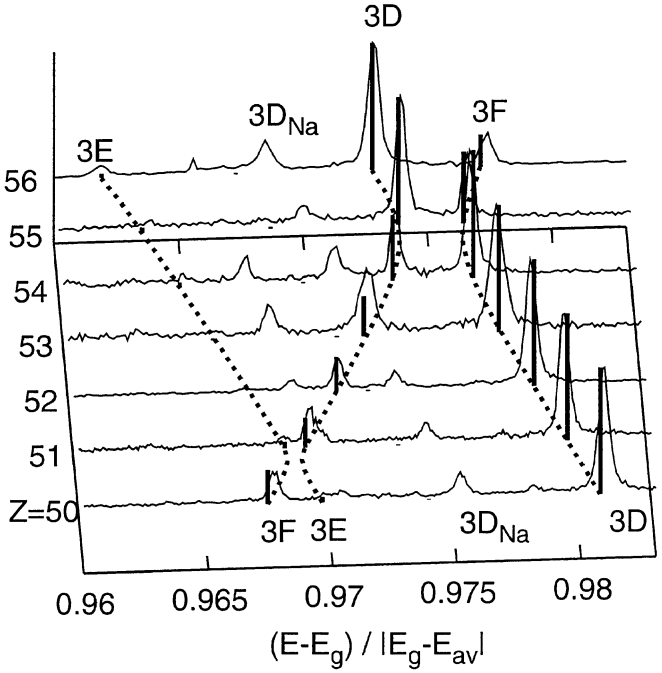

Fig. 3. 3-Dimension-plot of X-ray spectra for the neonlike sequence. Broken curves are calculations of energy levels, and solid impulses are calculations of line intensities obtained by the present CRM. The line intensities of 3D are normalized to unity. E_g and E_{av} represent the ground state energy and the configuration averaged energy in $(2l^{-1}3l')_{1-}$, respectively.

attributed to the weak configuration interaction between different K states, contrary to the large avoided crossing between the 3D and 3F energy levels that are due to the strong configuration interaction between the same K states. It is noted that there is still another unresolved weak but almost Z independent configuration interaction between $(2p^{-1}3d)\frac{3}{2}\left[\frac{1}{2}\right]_{1-}$, $(2p^{-1}3d)\frac{3}{2}\left[\frac{3}{2}\right]_{1-}$. In Fig. 5, the Z-dependence of intensity ratios for the three lines are shown. The present CRM consistently explains the intensity ratios for 3D/3F obtained by the experiments. Strong enhancement of the ratio is seen at $Z = 54 - 55$, which is due to redistribution of oscillator strengths and populations in the 3D and 3F levels through strong configuration mixing of $(2p^{-1}3d)\frac{3}{2}\left[\frac{1}{2}\right]_{1-}$ and $(2p^{-1}3s)\frac{1}{2}\left[\frac{1}{2}\right]_{1-}$. The present CRM predicts that the intensity ratio for 3E/3D decreases steeply and vanishes near $Z = 52$. Figure 6 shows the Z-dependence of reduced matrix elements of electric-dipole transitions multiplied by configuration mixing coefficients for the 3E level. Due to cancellation between the weighted reduced matrix elements for $(2p^{-1}3d)\frac{3}{2}\left[\frac{1}{2}\right]_{1-} \rightarrow (2p^6)_{0+}$ and $(2p^{-1}3d)\frac{3}{2}\left[\frac{3}{2}\right]_{1-} \rightarrow (2p^6)_{0+}$, the total reduced matrix element change its sing across the zero near $Z = 52$. The vanishing intensity of the 3E line is therefore attributed to the same mechanism with so-called Cooper-minimum for photo-

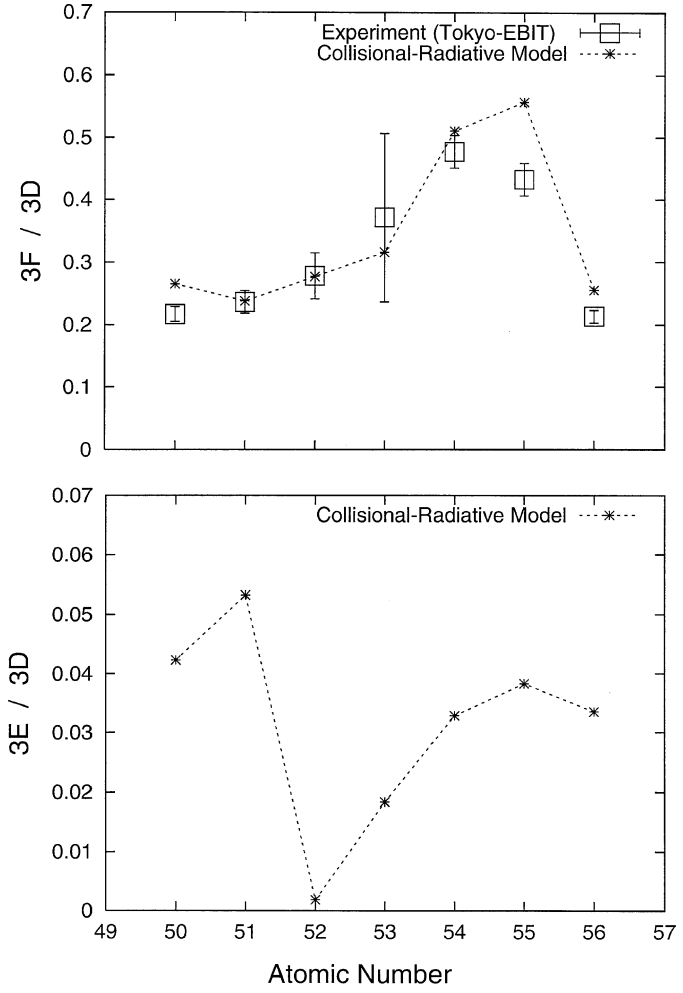

Fig. 5. Z-dependence of intensity ratios. The upper panel is the intensity ratio for 3F/3D, and the lower panel for 3E/3D.

ionzations of atoms. It is noted that a vanishing intensity of 3F near $Z = 58$ reported by Ivanova and Grant [5] is due to cancellation of the weighted reduced matrix elements for $(2p^{-1}3d)\frac{3}{2}[\frac{1}{2}]_{1-} \rightarrow (2p^6)_{0+}$ and $(2p^{-1}3s)\frac{1}{2}[\frac{1}{2}]_{1-} \rightarrow (2p^6)_{0+}$.

In summary, the present calculations for energies of the 3D, 3E and 3F lines of the neonlike highly charged ions were compared with RMBPT calculations and other available experiments as well as the experiments at the Tokyo-EBIT. Good agreement was obtained for $Z < 60$ with discrepancies of less than 0.04%, however considerable discrepancies between the two theories remains for very highly charge ions, probably due to some differences in the self-energy correction. Strong avoided crossing of the 3D and 3F levels was apparent near $Z = 55$ in both the experiments and calculations, contrary to the very weak avoided crossing of the 3E and 3F levels predicted near $Z = 51$ by the calculations. It turned out that they reflected the jK-coupling nature of relativistic atomic states for the 3D, 3E and 3F lines. The present CRM consistently explained the intensity ratios for 3F/3D obtained by the experiments for $Z = 50 - 56$. Both the experimental and CRM intensity ratios showed a significant enhancement at $Z = 54 - 55$.

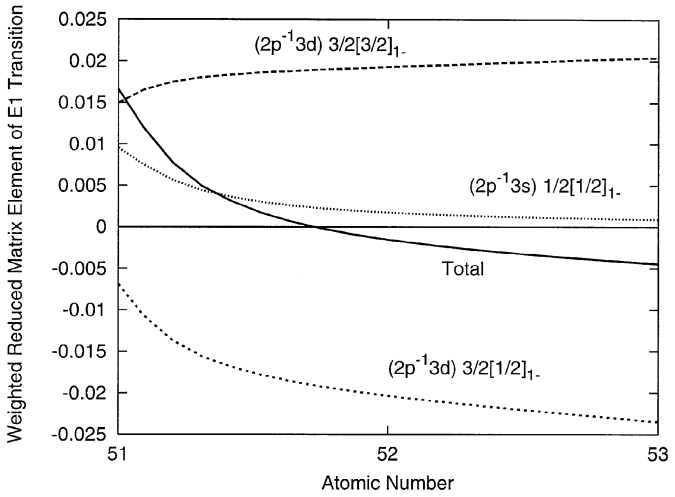

Fig. 6. Reduced matrix elements of electric-dipole transitions multiplied by configuration mixing coefficients for 3E.

The vanishing intensity of the 3E line near $Z = 52$ was predicted by the present CRM. The unraveled mechanism was the same as the so-called Cooper-minimum for photo-ionizations of atoms.

Acknowledgements

We owe it to collaborations with Kansai Research Establishment of Japan Atomic Energy Research Institute that calculations with the HULLAC code were permitted.

References

1. Weiss, A. W. and Kim, Y. -K., Phys. Rev. A **51**, 4487 (1995).
2. Kagawa, T., Honda, Y. and Kiyokawa, S., Phys. Rev. A **44**, 7092 (1991).
3. Beiersdorfer, P., AIP Conference Proceedings **274**, 365 (1993).
4. Rice, J. E. *et al.*, AIP Conference Proceedings **381**, 11 (1996).
5. Ivanova, E. P. and Grant, I. P., J. Phys. B **31**, 2871 (1998).
6. Kitano, E. and Kagawa, T., submitted to Phys. Rev. A.
7. Nakamura, N., Kato, D. and Ohtani, S., Phys. Rev. A **61**, 052510 (2000).
8. Loulergue, M. and Nussbaumer, H., Astron. Astrophys. **45**, 125 (1975).
9. Johnson, W. R. and Soff, G., At. Data Nucl. Data Tables **33**, 405 (1985).
10. Parpia, F. A., Fischer, C. F. and Grant, I. P., Comput. Phys. Commun. **94**, 249 (1996).
11. Avgoustoglou, E., Johnson, W. R., Liu, Z. W. and Sapirstein, J., Phys. Rev. A **51**, 1196 (1995); Avgoustoglou, E. and Liu, Z. W., Phys. Rev. A **54**, 1351 (1996).
12. Beiersdorfer, P. *et al.*, Phys. Rev. A **37**, 4153 (1988).
13. Chandler, G. A. *et al.*, Phys. Rev. A **39**, 565 (1990).
14. Dietrich, D. D. *et al.*, Phys. Rev. A **41**, 1450 (1990).
15. Hermann, G., J. Appl. Phys. **29**, 127 (1958).
16. Bar-Shalom, A., Klapisch, M., Goldstein, W. H. and Oreg, J., "The HULLAC Package Computer Set of Codes for Atomic Structure and Processes in Plasmas", (unpublished).
17. Press, W. H., Teukolsky, S. A., Vettering, W. T. and Flannery, B. P., "Numerical Recipes in FORTRAN", (Cambridge University Press, 1992), p. 51.
18. Cowan, R. D., "The Theory of Atomic Structure and Spectra", (University of California Press, 1981), p. 128.